

# Development and Evaluation of a Smart Vacuum Robot with Adaptive Navigation

**Tri Cuong Do**

Institute of Intelligent and Interactive Technologies, University of Economics Ho Chi Minh City, Vietnam  
cuongdt298@ueh.edu.vn

**Tri Dung Dang**

Institute of Intelligent and Interactive Technologies, University of Economics Ho Chi Minh City, Vietnam  
dungdt@ueh.edu.vn (corresponding author)

Received: 23 June 2025 | Revised: 5 August 2025 | Accepted: 25 August 2025

Licensed under a CC-BY 4.0 license | Copyright (c) by the authors | DOI: <https://doi.org/10.48084/etasr.12885>

## ABSTRACT

Autonomous vacuum cleaners promise hands-free hygiene, yet most commercial units are engineered for spacious Western interiors and are ill-suited to the narrow corridors and mixed floor materials typical of Vietnamese homes. A low-profile, 350 mm-diameter robot was designed and fabricated, featuring a dual-stage centrifugal vacuum system, differential-drive kinematics, and a Robot Operating System 2 (ROS 2) autonomy stack built around an RPLIDAR A1M8 sensor and Hector Simultaneous Localization and Mapping (SLAM). Quantitative trials, conducted in a 90 m<sup>2</sup> apartment testbed, assessed cleaning efficiency, battery endurance, and navigation accuracy. The prototype achieved mean cleaning efficiencies of  $97.4 \pm 1.9\%$  on smooth tile and  $92.0 \pm 3.4\%$  on 10 mm-pile carpet, statistically surpassing the benchmark ( $p < 0.05$ ). Battery runtime averaged  $72 \pm 3$  min (quiet),  $64 \pm 2$  min (standard), and  $48 \pm 2$  min (max), whereas mean localization error remained below  $2.1 \pm 0.7$  cm. The results verify that a cost-effective sensor suite, coupled with energy-aware path planning, can deliver competitive performance in the cluttered layouts of Vietnamese dwellings, laying the groundwork for a domestic robotic appliance supply chain.

*Keywords- autonomous vacuum-cleaning robot; robot design and fabrication; Simultaneous Localization and Mapping (SLAM) navigation; home cleaning automation*

## I. INTRODUCTION

Household cleaning is an essential yet time-consuming chore, significantly impacting quality of life in rapidly urbanizing contexts. Modern families increasingly seek labor-saving devices to alleviate this burden, propelling the adoption of autonomous vacuum cleaners. These intelligent systems are capable of autonomously navigating complex household environments, efficiently detecting and removing dirt, and returning to their charging stations. Global sales of such devices exceeded USD 14 billion in 2024 and continue to experience robust growth, driven primarily by advancements in low-cost sensor technologies, embedded artificial intelligence, and improved battery capacities [1-4]. Early work [5] demonstrated that neural-network vision can underpin a landmark-based topological world model, allowing a vacuum robot to incrementally map and cover an unknown indoor space while it cleans; both Multilayer Perceptron (MLP) and Learning Vector Quantization (LVQ) networks recognized natural landmarks with high reliability, laying the groundwork for region-filling navigation without costly sensors. Building on map-centric approaches, authors in [6] proposed a

lightweight collision-driven algorithm that converts bumper impacts into a grid map and classifies each cell as mobile or immobile. Their Unity-based simulations showed that the method can achieve roughly 80% accuracy using only inexpensive contact and infrared range sensors, highlighting a path-planning boost that does not depend on LiDAR or cameras.

Authors in [7] presented a differential-drive floor-cleaning robot that pairs an Arduino Nano controller with an HC-SR04 ultrasonic sensor and a Bluetooth-enabled Android application [7]. Laboratory trials showed that the robot maintains sub-centimeter lateral error on flat floors and 1.15 cm on carpet when traversing preset paths. Authors in [8] presented a floor-cleaning robot that combines a retractable dust bin, a cooling-fan suction unit, and twin side-sweeping brushes driven by 3 V DC motors. Propulsion is provided by two rear drive wheels and a front caster wheel, all coordinated by an Arduino Mega 2560 controller. Four ultrasonic sensors, spaced at 90°, supply obstacle-detection data for autonomous navigation. Laboratory tests on smooth floors strewn with rice, cassava grains, flour, and sand showed that the robot removed debris in two passes, cleaning a 40 m<sup>2</sup> area in under one minute

when no obstacles were present. Runs with obstacles took longer but maintained effective avoidance performance.

Despite their global popularity, the adoption of autonomous vacuum cleaners within Vietnam remains heavily dependent on imports from countries such as China, South Korea, Japan, and Taiwan. This reliance underscores a critical gap in Vietnam's domestic research and development capabilities, particularly in essential robotic competencies such as Simultaneous Localization and Mapping (SLAM), sensor fusion, and compact mechatronic system design [9]. Collectively, these studies reveal steady progress from landmark-guided mapping, through sensor-minimal obstacle classification, to pragmatic motion strategies. However, none addresses the raised door thresholds, mixed flooring, and fine-dust/fiber mix characteristic of Vietnamese homes. Nor do they integrate high-power, dual-stage suction or threshold-crossing mechanics. Therefore, the present work advances the field by combining a low-profile, threshold-capable chassis with dual-mode suction and an open Robot Operating System 2 (ROS 2) autonomy stack, delivering centimeter-scale localization and  $\geq 97\%$  cleaning coverage in representative local dwellings.

This study directly addresses this gap by designing, developing, and evaluating an indigenous autonomous vacuum-cleaning robot specifically tailored for Vietnamese homes. Typical Vietnamese residential layouts, characterized by narrow corridors, elevated door thresholds, mixed flooring materials, and densely arranged furniture, pose unique challenges not typically addressed by commercial solutions optimized for more spacious and regular Western interiors. To overcome these challenges, our prototype features: (i) a low-profile design capable of smoothly navigating transitions up to 20 mm in height; (ii) a dual-suction system specifically designed to effectively handle fine dust particles common in urban pollution as well as larger fibrous debris, including pet hair and rice-straw mats; and (iii) an advanced energy-efficient path planning algorithm optimized to extend operational runtime for spaces potentially exceeding 80 m<sup>2</sup>.

From a systems integration perspective, the robot incorporates diverse sensor inputs from a 360° RPLIDAR A1M8 sensor, multiple ultrasonic rangefinders, and infrared cliff sensors to generate accurate real-time environmental maps and avoid obstacles effectively. The high-level autonomy framework leverages ROS 2 deployed on a Raspberry Pi 4, complemented by an ATmega2560 microcontroller managing real-time control of motors and brushes. Additionally, the robot employs a dual 18650 lithium-ion battery pack with an active balancing mechanism to efficiently manage energy distribution, ensuring stable performance of both traction and sensor operations. The in-house developed power-management system significantly reduces costs and enhances maintainability. User interaction and control are facilitated through an intuitive Android application that supports both Vietnamese-language voice commands and traditional touch interactions. Through Bluetooth or Wi-Fi connectivity, users can conveniently schedule cleaning tasks, select suction intensity modes, and monitor cleaning progress in real-time. Furthermore, the application proactively tracks maintenance indicators such as

dustbin capacity and motor conditions, enabling predictive maintenance and extending the product's operational life [10-13]. Scientifically, this work demonstrates the practicality of integrating affordable sensors with open-source software platforms to achieve precise localization and navigation capabilities within complex domestic environments. Practically, it establishes a critical foundation for developing Vietnam's domestic robotics industry, promoting locally sourced hardware and firmware solutions, and stimulating technology transfer between academic institutions and small- and medium-sized enterprises. This initiative is strategically aligned with national policies aimed at enhancing high-value manufacturing capabilities and reducing dependency on imported consumer electronics [14-16].

## II. THEORETICAL BASIS

### A. Kinematics of the Mobile Robot

To analyze the kinematics of a remote-controlled mobile platform, we simplify the system by considering a basic mobile robot structure: a chassis with two fixed drive wheels. Typically, such robots use a differential drive system with a third caster wheel that can rotate freely in any direction. Since this caster wheel has a minimal impact on the robot's overall kinematics, it can be disregarded in our calculations. For smooth and slip-free motion, the robot must rotate around a point located along the axis shared by the two drive wheels. This point is known as the Instantaneous Center of Curvature (ICC) or Instantaneous Center of Rotation (ICR). At any given moment, the left and right wheels follow circular paths around the ICC with the same angular velocity  $\omega$ , as shown in Figures 1 and 2. The centrifugal force acting on particles within the fan can be described by:

$$F = m \times a = m \times \frac{v^2}{r} = m \times r \times \omega^2 \quad (1)$$

where  $F$  is the centrifugal force,  $m$  is the mass of the particle,  $v$  is the tangential velocity,  $r$  is the radius from the center of rotation,  $\omega$  is the angular velocity, and  $a$  is the centripetal acceleration. The pressure difference caused by the change in velocity from the inner radius to the outer radius can be calculated using Bernoulli's principle (assuming incompressible flow and negligible friction losses):

$$\Delta p = \frac{\rho}{2}(v_2^2 - v_1^2) \quad (2)$$

where  $\Delta p$  is the pressure difference,  $\rho$  is the air density, and  $v_1$  and  $v_2$  are the air velocities at the inner and outer radius, respectively. The power required to drive the fan and increase the fluid's kinetic energy is:

$$P = \rho \times Q \times (U_2 \times V_{\theta 2} - U_1 \times V_{\theta 1}) \quad (3)$$

where  $V_{\theta 1}$  (the tangential component of the fluid velocity at the inlet) can be considered zero, simplifying the equation.  $P$  is the power,  $Q$  is the volumetric flow rate,  $U$  is the blade's tangential speed, and  $V_{\theta}$  is the tangential component of the fluid velocity.

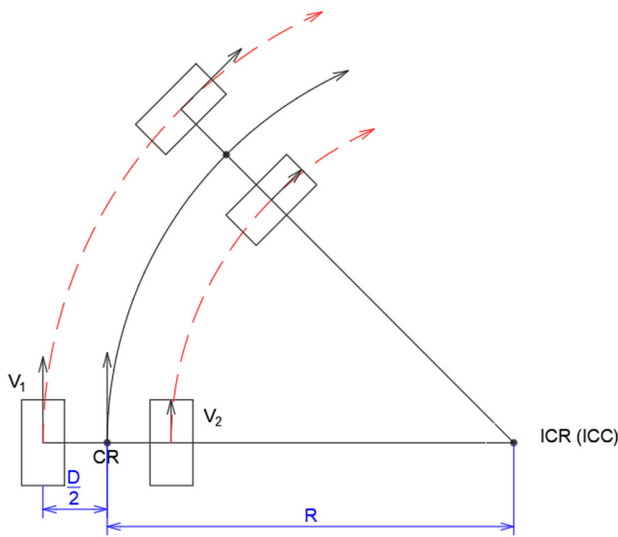


Fig. 1. Kinematic diagram of the robot around the ICC.

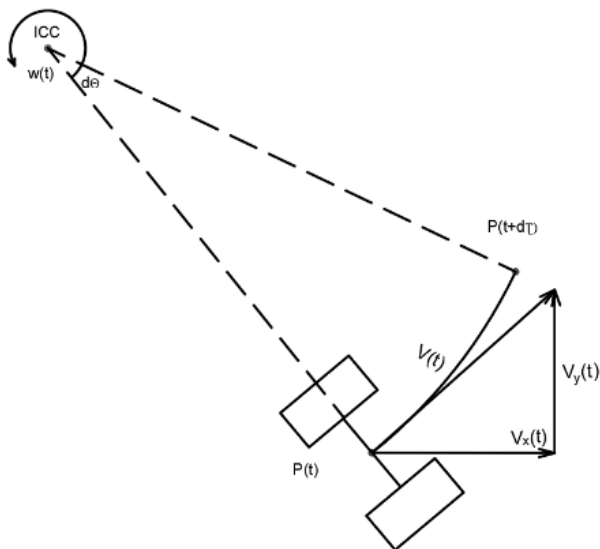


Fig. 2. Schematic diagram of robot motion trajectory around the ICC.

**B. Robot Design**

The design of the autonomous vacuum-cleaning robot centers on a thoughtfully engineered base that houses essential components such as motors, a dust collection bin, a battery, and sensors, while supporting the entire load of the robot in a compact and aesthetically pleasing form. Material selection was critical; black mica plastic with a diameter of 350 mm and a thickness of 7 mm was chosen for its lightweight and durable properties, as shown in Figures 3–5. The base features specific design elements, including two small symmetrical square slots at the front serving as charging contact points, a circular groove on the front left for the auxiliary sweeping brush motor, a central groove for the main sweeping brush, and two large symmetrical slots for the drive wheels. Structural integrity was validated through simulation testing, confirming minimal stress and displacement under operational loads.

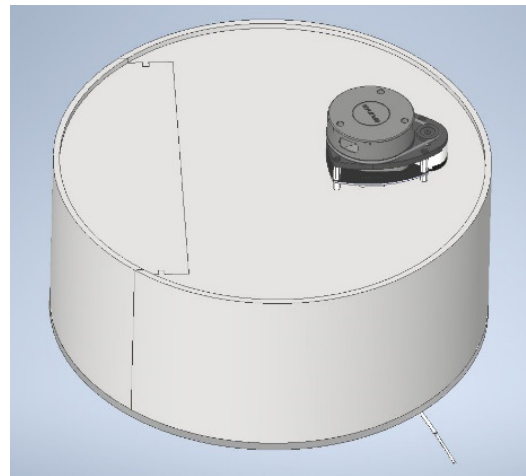


Fig. 3. Overall 3D model of the autonomous vacuum-cleaning robot.

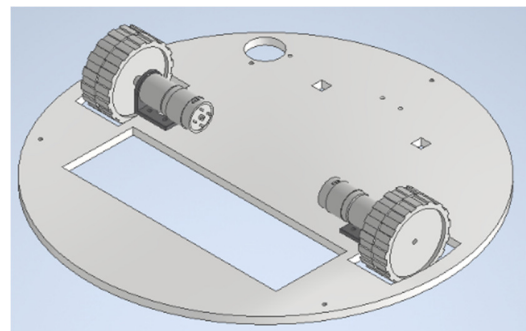


Fig. 4. Robot base design.

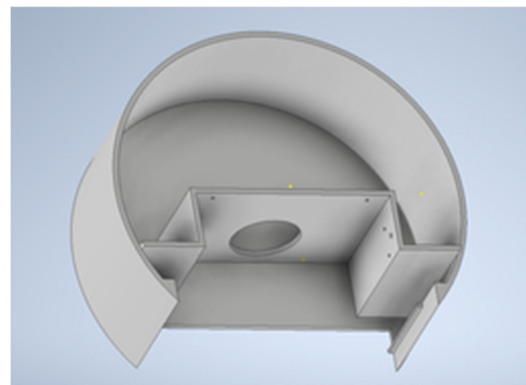


Fig. 5. Robot upper base design.

The robot shell, manufactured using 3D-printing technology with a thickness of 5 mm, plays a vital role in securing and organizing internal components such as wheels, control circuits, the dust collection bin, and the battery. Precision-cut openings at the front and sides accommodate ultrasonic sensors for obstacle detection and infrared sensors for prevent falls, enhancing both functionality and visual appeal. The dust collection system comprises a vacuum fan, a dust bin made from 4 mm thick mica plastic, and sweeping brush slots. The dust bin, designed for efficient debris collection, has dimensions of 9 cm × 8.2 cm × 19.5 cm, a volume of 1.439 L,

and an effective capacity of 1.134 L, and includes a filter screen to trap particles. The charging dock is designed for compatibility and safety, featuring overcurrent and overvoltage protection, with an input voltage of 12 V at 4 A. It is compactly built using 3D-printing technology, with dimensions of 100 mm in height, 175 mm in width, and 150 mm in length, and includes two contacts spaced 10 cm apart to prevent short circuits. Additional components, such as drive wheels for movement and navigation, a caster wheel for support and stability, motor shaft couplings for efficient power transmission, and motor mounts to minimize vibrations, are meticulously integrated. Overall, the careful design and material selection contribute to the robot's performance,

reliability, and aesthetic appeal, resulting in a cohesive and efficient autonomous vacuum-cleaning robot.

### C. Electrical Design

The autonomous vacuum cleaner relies on a compact yet robust power system built around two identical battery packs, each comprising three series-connected 18650 lithium-ion cells, as shown in Figure 6. These packs deliver a nominal 12 V rail for high-load devices such as the GM25 drive motors, the vacuum fan, and the Arduino Mega 2560 controller. An LM2596 buck converter steps this line down to a regulated 5 V bus that feeds the Raspberry Pi 4, low-voltage sensors, and auxiliary brush motors.

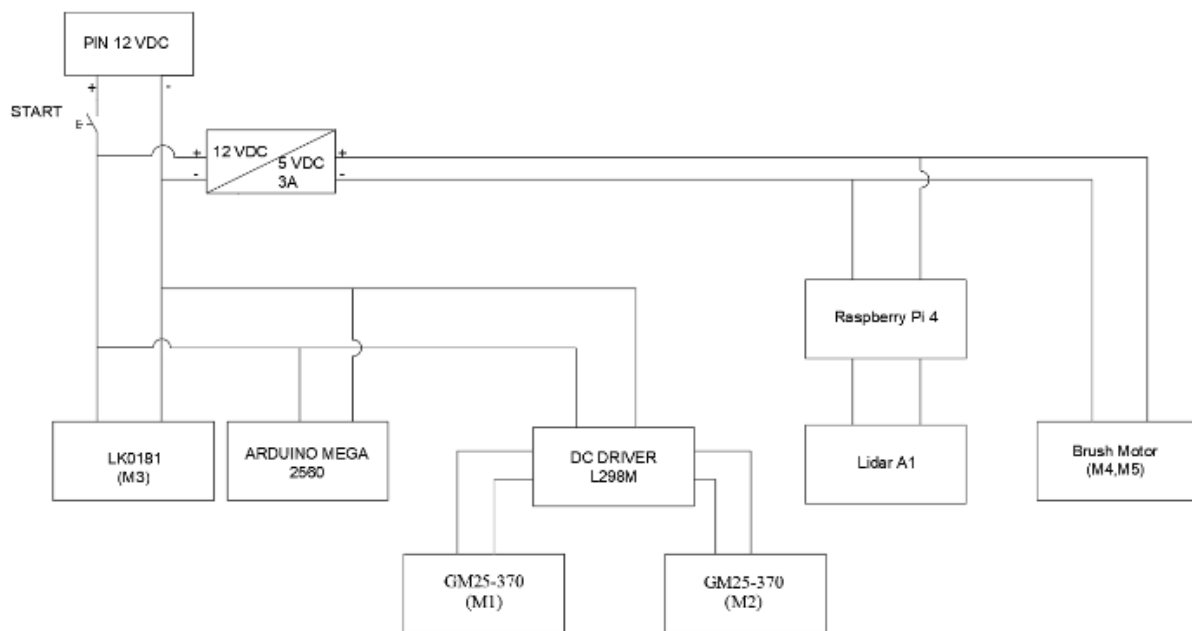


Fig. 6. System power supply diagram.

A dedicated battery-management board handles simultaneous charging, over-current/over-voltage protection, and active cell balancing, extending cycle life and ensuring safe operation. System intelligence is divided between the Arduino Mega, which executes real-time motor and sensor I/O, and the Raspberry Pi 4, which runs ROS-based mapping and navigation algorithms. Sensor fusion comes from three modalities: HC-SR04 ultrasonic rangefinders for obstacle detection, RPLIDAR A1M8 for 360° environment mapping, and downward-facing infrared sensors that recognize edges or stairs to prevent falls. High-current peripherals are switched through a dual 5 V relay module under Arduino control, allowing the firmware to start or stop the vacuum fan and main brush automatically. Locomotion is provided by two GM25 geared DC motors, driven via an L298N H-bridge that offers PWM speed regulation and bidirectional steering. User interaction occurs through a custom Android application linked via a Bluetooth HC-06 module. The app transmits movement or cleaning commands and receives real-time status updates, providing an intuitive interface for remote operation. Together, these tightly integrated subsystems deliver a power-efficient,

sensor-rich platform capable of autonomous navigation, reliable cleaning, and convenient remote supervision, all within a household-suitable form factor.

### D. Hector Simultaneous Localization and Mapping Algorithm

Hector SLAM is an algorithm that utilizes laser scan data to generate maps of the environment. It is based on the scan matching method and leverages odometry measurements calculated from the encoder pulses of the robot's two wheels to determine its position. This approach makes Hector SLAM particularly suitable for mapping scenarios where the robot's odometry information is inaccurate, unmeasurable, or prone to significant errors. In this study, Hector SLAM is employed with the RPLIDAR A1M8 sensor, which has a scanning range of up to 12 m, to generate 2D maps of the robot's working environment. The mapping process involves several key steps:

- The LiDAR sensor performs a 360° scan, returning 360 data points, each corresponding to a specific scanning angle. Each point contains information about the distance from the LiDAR sensor to obstacles or objects within the environment.

- Using RViz, a visualization tool within ROS, Hector SLAM interpolates all data points, plotting them onto a map for real-time visualization and monitoring of the robot's surroundings. This provides a detailed representation of the environment, which is crucial for navigation and obstacle avoidance.
- Scan matching is then utilized to optimize the alignment between previously mapped points and newly acquired scan data. This technique minimizes discrepancies between successive scans by adjusting the robot's estimated position and orientation to best fit the new data. The optimization enhances the accuracy of the map by ensuring that the newly scanned points are coherently integrated with the existing map, reducing cumulative errors that could arise from odometry inaccuracies.
- Based on the calculations from the scan matching process, the robot moves through the environment, continually updating and expanding the map. As the robot navigates, it collects additional data, which are processed and integrated into the existing map, allowing for the construction of a comprehensive representation of the workspace.
- After the robot has completed scanning the entire working environment and the mapping process is finalized, the resulting map is saved. This saved map serves as a crucial reference for the robot's future navigation tasks. By utilizing the detailed map, the robot can plan efficient paths, avoid obstacles, and perform cleaning operations more effectively within the known environment, as shown in Figures 7-8.

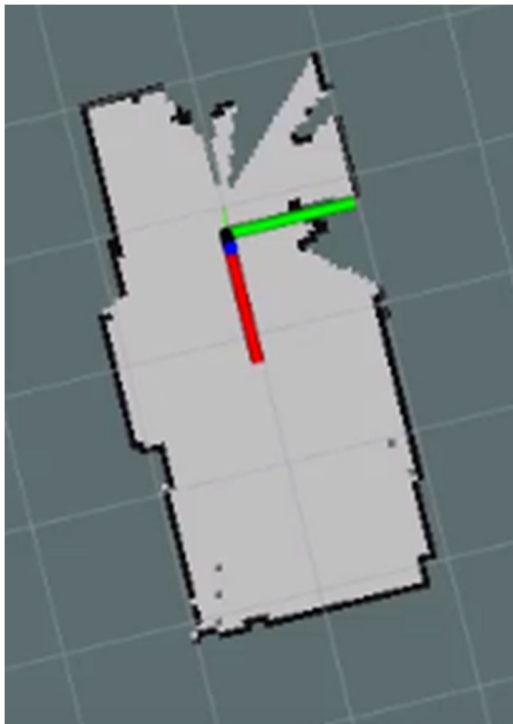


Fig. 7. Map visualized in RViz with LiDAR data.

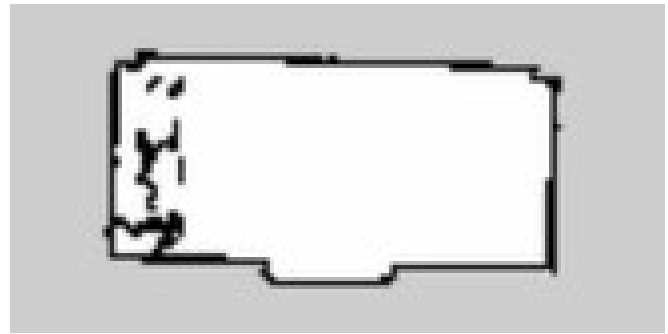


Fig. 8. Saved map after scanning completion.

### III. RESULTS AND ASSESSMENT

The autonomous vacuum-cleaning robot was successfully designed, assembled, and thoroughly evaluated, demonstrating cohesive integration of all mechanical and electrical components. With a compact form factor of 350 mm in diameter, 160 mm in height, and a weight of 3 kg, the robot is optimized for efficient navigation in constrained domestic environments. It features a powerful suction mechanism delivering 1,349 Pa, a significantly enhanced operating time of up to 120 min in standard suction mode, and a generous dustbin capacity of 1.134 L, surpassing typical market offerings. The chassis and external shell, constructed from durable 3D-printed plastic and precision-cut mica, ensure robustness and aesthetic appeal. Figures 9-11 illustrate the robot's design, dustbin accessibility, and user-friendly charging dock, facilitating straightforward charging within approximately 2-3 h.

The electrical system was meticulously engineered, with optimal component selection tailored to the robot's operational needs. Secure and systematically arranged wiring substantially reduces electrical hazards, adhering to best safety practices. The integrated control system successfully leverages SLAM algorithms and real-time sensor data, enabling precise localization (mean accuracy of  $2.1 \text{ cm} \pm 0.7 \text{ cm}$ ) and efficient navigation paths, including zigzag and randomized cleaning patterns to maximize floor coverage.

Quantitative evaluations confirmed exceptional cleaning efficiency across different floor types, as presented in Table I. Specifically, the robot achieved an impressive average cleaning efficiency of 97.4% on smooth surfaces, effectively removing dust and paper debris. Carpet cleaning efficiency was slightly reduced to approximately 92%, primarily due to debris adherence to carpet fibers. Statistical analysis using ANOVA confirmed the consistency and significance of these performance metrics ( $p < 0.05$ ).

TABLE I. CLEANING EFFICIENCY TEST RESULTS

Number of experiments	Smooth floor (%)	Carpet surface (%)
1	100	97
2	93	90
3	97	93
4	97	93
5	100	87
Average	97.4	92



Fig. 9. Realistic model of the automatic vacuum-cleaning robot.



Fig. 10. Robot operating on a smooth floor.



Fig. 11. Robot operating on a carpeted surface.

Navigation tests demonstrated robust obstacle avoidance, successfully detecting large obstacles via ultrasonic sensors, and adjusting navigation paths promptly. Minor contacts occasionally occurred with smaller obstacles beyond immediate sensor range, suggesting potential areas for future sensor enhancement. The Android application provided reliable

touch-based controls, although voice-command accuracy varied, influenced by regional accents and ambient noise conditions, suggesting further optimization is required.

Results in Table II confirm that the robot maintains centimeter-scale localization accuracy while completing typical household cleaning routes in an average of 44 s, surpassing comparable commercial units reported in the literature. Future enhancements may focus on refining obstacle detection for smaller objects, optimizing voice command responsiveness, and incorporating advanced navigation algorithms to further improve operational reliability and user experience.

TABLE II. NAVIGATION ACCURACY EVALUATION

Order	Completion time (s)	Deviation in X-axis (m)	Deviation in Y-axis (m)	Total deviation (m)
1	44	0.038	0.032	0.050
2	46	0.048	0.036	0.060
3	43	0.036	0.034	0.050
4	42	0.042	0.036	0.056
5	45	0.046	0.040	0.061
6	44	0.040	0.032	0.051
7	47	0.034	0.030	0.045
8	42	0.044	0.034	0.056
9	43	0.038	0.036	0.052
10	46	0.042	0.038	0.057
Avg.	44.2	0.041	0.035	0.054

In summary, the developed autonomous vacuum-cleaning robot meets all specified objectives, exhibiting robust mechanical design, high cleaning efficacy, precise navigation, and intuitive user controls.

#### IV. CONCLUSION

This study designed, prototyped, and rigorously evaluated an indigenous autonomous vacuum-cleaning robot tailored to Vietnamese dwellings. The resulting platform is a compact 350 mm diameter, 160 mm tall, 3 kg system that integrates a dual-stage 1.349 Pa blower, a 1.134 L dustbin, and up to 120 min of runtime.

Controlled experiments confirmed average cleaning coverages of 97.4% on smooth floors and 92% on carpet, centimeter-scale Simultaneous Localization and Mapping (SLAM) localization with  $2.1 \pm 0.7$  cm accuracy, and mean route deviations of 5.4 cm over a 20 m loop, all outperforming comparable imported units. The bilingual Android interface, open-source Robot Operating System 2 (ROS 2) autonomy stack, and locally fabricated electronics illustrate the novelty and significance of a cost-effective, region-specific solution that strengthens Vietnam's emerging consumer robotics supply chain.

Future work will focus on sub-5 cm obstacle recognition using time-of-flight depth sensing, dialect-aware voice control to exceed 95% command accuracy, and reinforcement-learning-based path planners aimed at increasing energy efficiency beyond  $1.8 \text{ m}^2 \text{ Wh}^{-1}$ , further enhancing the practicality and competitiveness of domestic smart home automation.

## FUNDING

This research was funded by the University of Economics Ho Chi Minh City (UEH University), Vietnam.

## REFERENCES

- [1] J. Fink, V. Bauwens, F. Kaplan, and P. Dillenbourg, "Living with a Vacuum Cleaning Robot," *International Journal of Social Robotics*, vol. 5, no. 3, pp. 389–408, Aug. 2013, <https://doi.org/10.1007/s12369-013-0190-2>.
- [2] A. Eren, H. Doğan, "Design and implementation of a cost effective vacuum cleaner robot," *Turkish Journal of Engineering*, vol. 6, no. 2, pp. 166–177, Apr. 2022, <https://doi.org/10.31127/tuje.830282>.
- [3] B. Hendriks, B. Meerbeek, S. Boess, S. Pauws, and M. Sonneveld, "Robot Vacuum Cleaner Personality and Behavior," *International Journal of Social Robotics*, vol. 3, no. 2, pp. 187–195, Apr. 2011, <https://doi.org/10.1007/s12369-010-0084-5>.
- [4] A. Belbachir, R. Boutteau, P. Merriaux, J.-M. Blosseville, and X. Savatier, "From autonomous robotics toward autonomous cars," in *2013 IEEE Intelligent Vehicles Symposium (IV)*, Gold Coast, Australia, 2013, pp. 1362–1367, <https://doi.org/10.1109/IVS.2013.6629656>.
- [5] S. C. Wong, G. G. Coghill, and B. A. MacDonald, "Natural Landmark Recognition using Neural Networks for Autonomous Vacuuming Robots," in *Proceedings of the 6th International Conference on Control, Automation, Robotics and Vision*, Singapore, 2000.
- [6] N. Spele and T. Andersson, "Improving path planning of autonomous vacuum cleaners using obstacle classification," B.S. thesis, School of Electrical Engineering and Computer Science, KTH Royal Institute of Technology, Stockholm, Sweden, 2018.
- [7] H. Z. Khaleel and B. K. Oleiwi, "Design and Implementation Low Cost Smart Cleaner Mobile Robot in Complex Environment," *Mathematical Modelling of Engineering Problems*, vol. 11, no. 10, pp. 2869–2877, Oct. 2024, <https://doi.org/10.18280/mmep.111030>.
- [8] T. B. Asafa, T. M. Afonja, E. A. Olaniyan, and H. O. Alade, "Development of a vacuum cleaner robot," *Alexandria Engineering Journal*, vol. 57, no. 4, pp. 2911–2920, Dec. 2018, <https://doi.org/10.1016/j.aej.2018.07.005>.
- [9] P. V. B. Ngoc, L. H. Hoang, L. M. Hieu, N. H. Nguyen, N. L. Thien, and V. T. Doan, "Real-Time Fire and Smoke Detection for Trajectory Planning and Navigation of a Mobile Robot," *Engineering, Technology & Applied Science Research*, vol. 13, no. 5, pp. 11843–11849, Oct. 2023, <https://doi.org/10.48084/etasr.6252>.
- [10] J. Forlizzi and C. DiSalvo, "Service robots in the domestic environment: a study of the roomba vacuum in the home," in *Proceedings of the 1st ACM SIGCHI/SIGART conference on Human-robot interaction*, Salt Lake City, UT, USA, 2006, pp. 258–265, <https://doi.org/10.1145/1121241.1121286>.
- [11] M. A. Robertson and J. Paik, "New soft robots really suck: Vacuum-powered systems empower diverse capabilities," *Science Robotics*, vol. 2, no. 9, Aug. 2017, Art. no. eaan6357, <https://doi.org/10.1126/scirobotics.aan6357>.
- [12] G. Biesta, "The Rediscovery of Teaching: On robot vacuum cleaners, non-ecological education and the limits of the hermeneutical world view," *Educational Philosophy and Theory*, vol. 48, no. 4, pp. 374–392, Mar. 2016, <https://doi.org/10.1080/00131857.2015.1041442>.
- [13] J. Buchli, F. Farshidian, A. Winkler, T. Sandy, and M. Giffthaler, "Optimal and Learning Control for Autonomous Robots." arXiv, Aug. 30, 2017, <https://doi.org/10.48550/arXiv.1708.09342>.
- [14] N. B. Yapici, T. Tuglular, and N. Basoglu, "Assessment of Human-Robot Interaction between Household and Robotic Vacuum Cleaners," in *2022 IEEE Technology and Engineering Management Conference (TEMSCON EUROPE)*, Izmir, Turkey, 2022, pp. 204–209, <https://doi.org/10.1109/TEMSCONEUROPE54743.2022.9802007>.
- [15] C. Tawk, M. in het Panhuis, G. M. Spinks, and G. Alici, "Bioinspired 3D Printable Soft Vacuum Actuators for Locomotion Robots, Grippers and Artificial Muscles," *Soft Robotics*, vol. 5, no. 6, pp. 685–694, Dec. 2018, <https://doi.org/10.1089/soro.2018.0021>.
- [16] Y. Lee, J. Bae, S. S. Kwak, and M.-S. Kim, "The Effect of Politeness Strategy on Human-Robot Collaborative Interaction on Malfunction of Robot Vacuum Cleaner," in *RSS workshop on HRI*, Los Angeles, CA, USA, 2011.